Jurnal Ilmu Fisika
Vol. 16, No. 2, September 2024, pp. 151–165
ISSN: 1979-4657 (Print); 2614-7386 (Online)
https://doi.org/10.25077/jif.16.2.151-165.2024

Jurnal Ilmu Fisika
Open Access

Annual and Interannual Rainfall Variability in Indonesia Using Empirical Orthogonal Function (EOF) Analysis and Its Response to Ocean-Atmosphere Dynamics

Melly Ariska[1], Suhadi Suhadi[2], Supari Supari[3], Muhammad Irfan[4], Iskhaq Iskandar[4]

[1] Mathematical Sciences and Natural Sciences, Universitas Sriwijaya, Palembang, 30662, Indonesia
[2] Department of Physics Education, Universitas Islam Negeri Raden Fatah, Palembang, 30126, Indonesia
[3] Meteorology Climatology and Geophysics Agency, 3540 Indonesia
[4] Department of Physics, Universitas Sriwijaya, Palembang, 30662, Indonesia

Article Info

Article History:

Received May 01, 2024
Revised July 24, 2024
Accepted July 28, 2024
Published online August 15, 2024

Keywords:

Rainfall
Ocean-Atmosphere Dynamics
EOF
Annual
Interannual
Rainfall Variability

Corresponding Author:

Iskhaq Iskandar,
Email: iskhaq_iskandar@gmail.com

ABSTRACT

We investigate rainfall variability in Indonesia using the Empirical Orthogonal Function (EOF) method. The analysis starts by taking three main modes of EOF results, namely EOF1, EOF2, and EOF3. The EOF1 region is southern Indonesia, from southern Sumatra to Timor Island, parts of Kalimantan, parts of Sulawesi, and parts of Irian Jaya. The EOF2 region is located in northwestern Indonesia and includes the northern part of Sumatra and the northwestern part of Kalimantan. The EOF3 region covers Maluku. This study aims to analyze the annual and inter-annual variability of rainfall in anticipation of the threat of hydrometeorological disasters. Based on the correlation value of the principal component (PC) with the dipole mode index (DMI) and Niño3.4 index, it has a period similar to El Niño-Southern Oscillation (ENSO) and Indian Ocean Dipole (IOD). Rainfall in Indonesia is very sensitive to sea surface temperature (SST) in the southeastern Indian Ocean and the central Pacific Ocean, which means that rainfall patterns in Indonesia can change significantly if SST in the region changes.

1. INTRODUCTION

Rainfall was one of the atmospheric parameters that is difficult to predict due to its large spatial and temporal variability, especially in tropical maritime patterns such as Indonesia (Yamanaka, 2016). Indonesia's long coastline and mountainous terrain have an impact on air currents, weather changes, climate, and rainfall. In addition, Indonesia has small variations in temperature and large variations in rainfall (Suhadi et al., 2023). As an archipelago, Indonesia has three rainfall patterns: monsoon, equatorial, and local. Each rainfall pattern has its own characteristics and causes. The most dominant pattern is the monsoon pattern, which was a twelve-month rain cycle consisting of one rainy season and one dry season (Aldrian & Dwi Susanto, 2003). This is influenced by the monsoon winds that blow from the northern to southern hemisphere due to differences in air pressure caused by the apparent motion of the sun. In addition, some areas in Indonesia also have an equatorial pattern that is characterized by

having two rainy seasons or a six-month rainy period. The equatorial pattern is influenced by the revolutionary motion of the earth around the sun and the influence of the convergence zone on rain (Inter Tropical Convergence Zone). Meanwhile, local rainfall patterns are caused by an area's topography and environmental conditions.

The role of rainfall is critical in shaping the hydrological and ecological dynamics of regions throughout the world, having a significant impact on water resources, agriculture, infrastructure, and ecosystems (Y. Hamada et al., 2016). The Indonesian archipelago is no exception to being affected by climate change, which is increasingly worrying. Indonesia is located in the equatorial belt, so it has a tropical climate characterized by high rainfall variability, with rainfall patterns greatly influencing the socio-economic and environmental landscape (Putra et al., 2019). Therefore, understanding the variability of rainfall patterns in Indonesia is critical for effective water resource management, disaster preparedness, and sustainable development initiatives.

Over the past few decades, greater attention has been devoted to studying climate variability and its implications for regions globally (Tavakol et al., 2020). Hydrometeorological disasters can trigger floods, landslides, and other natural disasters. The need for a comprehensive analysis of the observed trends in rainfall events is urgent. The analysis provides valuable insight into changing climate conditions and their potential consequences for society. Despite the importance of understanding the variability of rainfall patterns in Indonesia, only a few studies have explicitly focused on the topic of mapping rainfall areas spatially and temporally and analyzing how much they influence the dynamics of the surrounding Indo-Pacific oceans. Existing research often does not examine long-term trends comprehensively and only focuses on short-term analysis or specific events (Field et al., 2016; Sprintall et al., 1999).

The parameters of Indo-Pacific tropical climate modes are important to observe to see the ocean-atmosphere interactions that affect climate patterns in the surrounding area, especially Indonesian waters. Westerlies and easterlies strongly influence Indo-Pacific tropical climate patterns and also have a global impact as evidenced by rainfall in various parts of the world (Horii et al., 2022; Lestari et al., 2019). This global teleconnection is linked to annual tropical-Indian-Pacific interactions in the atmosphere, namely the Indian Ocean Dipole (IOD) in the tropical Indian Ocean and the El Niño Southern Oscillation (ENSO) in the equatorial Pacific. The IOD phenomenon is the main cause of Indian Ocean tropical climate variability anomalies (Landsea & Knaff, 2000). The positive phase of the IOD event is characterized by low sea surface temperature anomalies in the southeastern Indian Ocean and high SST anomalies in the central and northwestern Indian Ocean. These anomalies are associated with easterly wind anomalies along the equator and southeasterly wind anomalies along the west coast of Sumatra and near southern Java. Changes in ocean and atmospheric circulation in turn move warm water from the basin in the eastern Indian Ocean into the central/western Indian Ocean and then into the eastern Indian Ocean tropics. In addition, these changes suppress atmospheric convection over the warm water pool in the eastern Indian Ocean, while atmospheric convection increases over the western and central Indian Ocean (Irfan & Iskandar, 2022; Lestari et al., 2019; Mason & Mimmack, 2002). This phenomenon led to increased moisture in East Africa and South Asia and severe drought in India and Australia. ENSO-induced droughts on maritime continents can increase positive IOD events (Suhadi et al., 2023). Meanwhile, ENSO events consist of ocean-atmosphere interactions in the equatorial Pacific (Field et al., 2016; Sprintall et al., 1999).

ENSO and IOD are Indo-Pacific climate modes that receive a lot of global attention today because of their impact on climate change in a region, especially Indonesia. ENSO is expressed as annual changes in ocean and sea surface temperatures in the equatorial Pacific. Previous research shows that ENSO has environmental and socio-economic impacts around the world (Hendon, 2003b; Lestari et al., 2018). Rainfall anomalies in Indonesia are strongly correlated with ENSO. ENSO causes changes in rainfall, surface air temperature, agricultural production and disease outbreaks in many parts of the world. El Niño often causes drought conditions in continental maritime Indonesia, leading to large forest and peat fires, air pollution and haze as observed in the 1994 and 1997/98 El Niño events (Mason & Mimmack, 2002). Hamada et al., (2002) noted that the rainy season tends to be late (early) in the Indonesian pattern in El Niño (La Niña) years, decreasing (increasing) the amount of rainfall in

Indonesia (Hendon, 2003b). The negative correlation with the ENSO is particularly high in the eastern part of the maritime continent during the northern summer and autumn (dry and transitional seasons) (Ashok et al., 2003; Irfan & Iskandar, 2022; Mason & Mimmack, 2002). The IOD is also thought to have a major influence on rainfall impacts on maritime continents (Iskandar et al., 2008; Saji & Vinayachandran, 1999).

Ashok et al. (2003) described Sea Surface Temperature (SST) cooling anomalies caused by the IOD off the coasts of Java and Sumatra as causing unnatural land subsidence in the maritime continents during the summer to autumn period of the northern hemisphere. This phase results in reduced rainfall across Indonesia (Iskandar et al., 2022; Lestari et al., 2019). Extreme events such as high Citarum river flows in northwest Java tend to occur under La Niña conditions, while low river flows occur during positive phase IOD events (Y. Hamada et al., 2016). Their study focussed on river flow events, not localised rainfall, but provided clues as to what is the typical response of Indonesian rainfall to IOD and ENSO (Chang et al., 2004). This phenomenon motivates researchers to investigate the impact of ENSO and IOD on annual and interannual rainfall variability in the Indonesian pattern in detail and more depth by using rainfall data over a longer period from 1948 to 2016.

The identification of rainfall areas requires an appropriate method to observe its patterns and characteristics. Aldrian (2001) used the double correlation method which resulted in five climatic patterns in Indonesia. (Iskandar et al., 2022)used the SVD method in mapping rainfall in Indonesia, while Jun-Ichi et al., (2012) used Fourier transformation to analyze the series of rainfall areas in Indonesia. The identification of rainfall areas that have been done before is only limited to showing the division of areas based on the statistical methods used, but has not explained in detail the ocean-atmosphere dynamics that affect it. In this research, the method used is Empirical Orthogonal Function (EOF) which is a method to determine the dominant patterns determined by the data and evolve in space and time (Hendon, 2003a). The EOF method is used to look at the spatial and temporal patterns of the Indonesian Pattern, which is expected to extract information directly from rainfall data to identify the period of atmospheric phenomena recorded in the data. This article analyses rainfall variability using the EOF method and examines the extent to which the equatorial sea surface temperature phenomenon of the Indian and Pacific oceans affects rainfall in Indonesia. The purpose of the study is to analyze in depth and comprehensively the annual and interannual variability of spatial and temporal distribution of rainfall in Indonesia by EOF method under the influence of SST and wind (Iskandar et al., 2017).

Recent satellite observations have revealed large-scale variability in rainfall patterns on an annual basis. However, the resolution of spatial-temporal visualizations produced in previous studies have not considered regional topographic conditions to determine the local impact and relationship between rainfall in Indonesia and the Indo-Pacific climate mode (ENSO/IOD). Therefore, researchers are motivated to analyse rainfall variability in Indonesia and relate it to SST along the equator of the Pacific Ocean and Indian Ocean. The results of this research are expected to contribute to various scientific fields that have a close relationship with efforts to anticipate hydrometeorological disasters with the results in the form of mapping annual and interannual rainfall patterns. This comprehensive study is expected that the results obtained will be able to describe the annual and interannual rainfall patterns in the Indonesian region properly and accurately.

2. METHOD

Monthly rainfall data covering the period January 1948 to December 2016 with a horizontal resolution of 0.250 x 0.250 is taken from Monthly Precipitation data from Princeton University. In addition to rainfall data, this study also uses monthly zonal wind (u10), meridional wind (v10), vertical velocity and SST data from ERA5 monthly averaged data link https://cds.climate.copernicus.eu/. Dipole Mode Index (DMI) and Niño3.4 Index from National Oceanic and Atmospheric Administration (NOAA) with link https://psl.noaa.gov/. Rainfall data obtained from Monthly Precipitation from Princeton University is a highly variable and fluctuating monthly rainfall data. This rainfall dataset has a high spatial-temporal resolution allowing us to investigate the impact of ENSO/IOD on annual and interannual rainfall variability based on the division of rainfall patterns from the EOF method analysis.

One of the objectives of the EOF analysis of these observations is to determine the dominant patterns and eliminate the correlation between the data to obtain the maximum possible diversity of the original data with as few principal components as possible.

The principal component is the result of EOF analysis transformation with a certain diversity value. In this study, the data used is re-analysis data. According Yamanaka, (2018), the use of re-analysis data is so that each variable at each point has the same importance in representing the overall data. There are many criteria for selecting the number of principal components included in the EOF analysis, but in this study, the number of principal components used is seen from the percentage of cumulative variance. According to Kajita et al., (2022) the main component is only included if it has a proportion of cumulative variance of more than 50%. According to Yamanaka, (2016) areas with large variability should dominate in EOF analysis and are important contributors to excess or deficiency of rainfall (Ardiani, 2013; Ramage, 1968). In the EOF analysis, the correlation of the new variables of the first principal component, EOF1, is orthogonal to the second principal component, EOF2, making each origin variable maximal in the second principal component, so that the total contribution of each origin variable is made intermediate.

EOF is a method to determine the dominant patterns determined by the data and evolve in space and time. Aldrian & Dwi Susanto (2003) explained that the main objective of EOF analysis is to reduce a large number of data variables to only a few variables without changing most of the variance of the original data. The EOF analysis begins by determining the covariance matrix of the constructed rainfall data matrix, i.e., the covariance matrix:

$$\sum = \frac{1}{n-1} X^T X. \tag{1}$$

The covariance matrix $\sum$ in Equation (1) is a real symmetric matrix that has eigenvectors $e_m(x, y)$ and positive eigenvalues λ_m. By using EVP, the following formula is obtained:

$$Re_m = \lambda_m e_m. \tag{2}$$

From Equation (2), the eigenvalue λ and the eigenvector e are obtained which satisfy the equations $|R - \lambda I| = 0$ and $(R - \lambda I)e = 0$. The eigenvector $e_m(x, y)$ is an orthogonal EOF temporal variability, thus satisfying the equation (Pourasghar et al., 2012):

$$\sum_{x,y=1}^{N} e_m\,(x_i, y_i) e_n\,(x_i, y_i) = 0, m \neq n. \tag{3}$$

The EOF temporal variability in Equation (3) is mounded to obtain a new equation. The new equation is the spatial variability $u_m(t)$ obtained by projecting the original data on the temporal variability. Singleton defines it as the multiplication of the eigenvector $u_m(x, y)$ with the initial data matrix $X(s, t)$, namely:

$$u_m(t) = \sum_{x,y=1}^{N} X\,(x, y, t) e_m(x, y). \tag{4}$$

Variants The variance explained by the n_{th}-sized variable in Equation (4) depends on the percentage contribution p_m of each eigenvalue (Equation (5)).

$$p_m = \frac{\lambda_m}{\sum_{n=1}^{N} \lambda_n}. \tag{5}$$

The EOF method is capable of extracting principal components (PCs) from patterns in time series. Each PC is orthogonal to the others (Aldrian, 2001; Aldrian & Dwi Susanto, 2003). The first PC (PC1) will be the most dominant pattern and explain most of the variance. Then PC2 will be the second most dominant PC, followed by PC3, and so on. In total, there will be a number of PCs equal to the amount of data in the time series. The original data set will be a combination of all the PCs multiplied by the time series of their respective coefficients time series. According to J.-I. Hamada et al. (2012) stated that rainfall fluctuations at the beginning of the rainy season in November-December-January (NDJ) and the end of the dry season in August-September-October (ASO) indicate the influence of ENSO dynamics centered in the Pacific Ocean and IOD centered in the Indian Ocean as evidenced by

the analysis of rainfall trends in the Indonesian region showing a significant increase (decrease) during the years of the ENSO and IOD phenomena.

The data of these hydrometeorological parameters were correlated with the eigenvector coefficients of the annual and interannual analyses. The correlation used is a linear correlation between two variables, known as Pearson's correlation. The following formula is used to calculate the correlation:

$$r = \frac{n\sum_{i=1}^{n} x_i y_i - (\sum_{i=1}^{n} x_i)(\sum_{i=1}^{n} y_i)}{\sqrt{\left[n\sum_{i=1}^{n} x_i^2 - (\sum_{i=1}^{n} x_i)^2\right]\left[n\sum_{i=1}^{n} y_i^2 - (\sum_{i=1}^{n} y_i)^2\right]}}. \quad (6)$$

Furthermore, to confirm the level of statistical significance, a t-test was calculated. The t-test is one of the statistical tests used to test the truth of a hypothesis stating that between two samples taken from the same population there is no significant difference.

3. RESULTS AND DISCUSSION

3.1 Spatial and Temporal Patterns of Rainfall

The spatial patterns of EOF1, EOF2 and EOF3 are given in Figure 1. EOF1, EOF2 and EOF3 explain 39.17%, 20.9% and 8.82% of all variances respectively. The three PCs have explained more than half of the total variance of the entire data set over 69 years or 828 months.

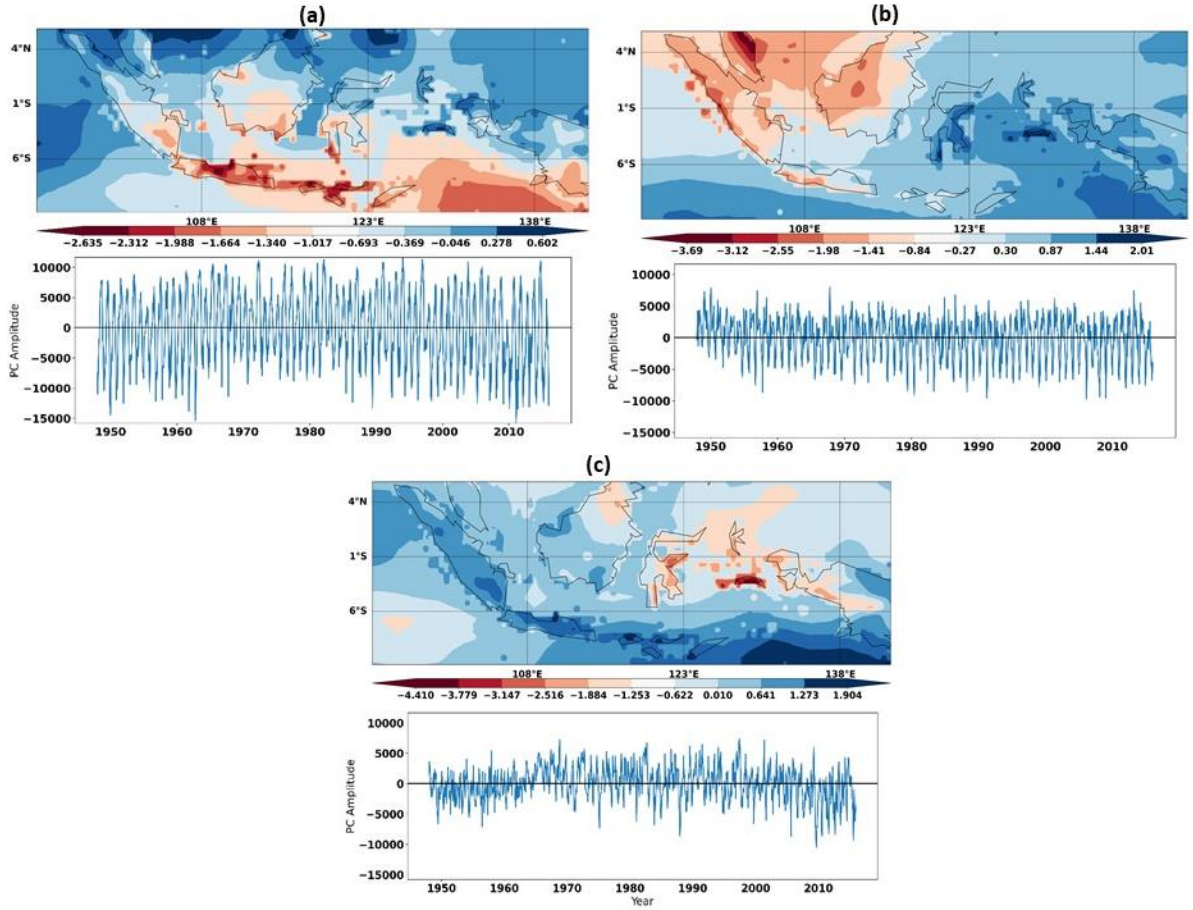

Figure 1 Mapping results based on EOF method and time series of EOF1 (a), EOF2 (b), and EOF3 (c).

Based on Figure 1, each EOF pattern has its own characteristics. The EOF1 pattern was aligned with the monsoon pattern of Aldrian & Dwi Susanto (2003) which has a strong influence from two monsoons, namely the wet northwest monsoon from November to March (NDJFM) and the dry

southeast monsoon from May to September (MJJAS). Then, the EOF2 pattern which is an equatorial pattern associated with the southern and northern movements of the ITCZ and the EOF3 pattern which is a localized pattern. Figure 2 and Figure 3 describe the climatology and periodograms of the three main patterns of the EOF mode.

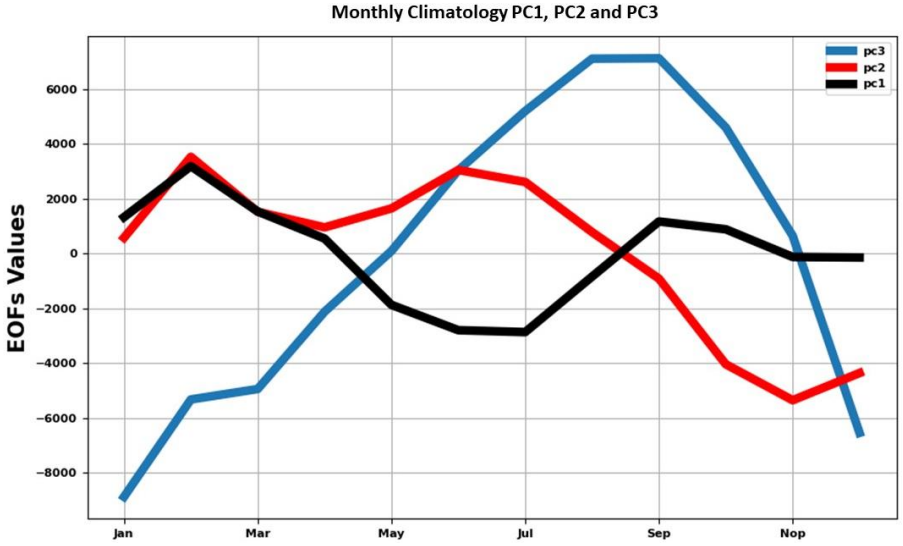

Figure 2 Climatology of EOF1, EOF2, and EOF3.

The climatology of the EOF1 region has one rainfall peak and one valley, the EOF2 region has two peaks, namely in October–November (ON) and March to May (MAM) and the EOF3 region has two peaks in the middle of the year (JJ) and the end of the year (NDJ), which differs from the other two regions in having a peak near the end/beginning of the year. The periodogram of each PC is investigated to clarify which frequency dominates the rainfall pattern in each pattern from each main coefficient of the generated EOF mode.

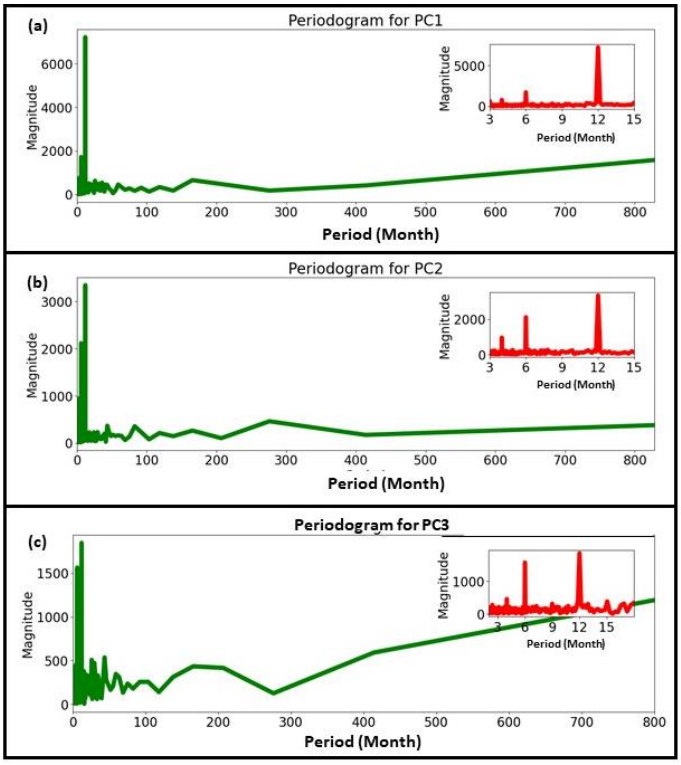

Figure 3 FFT periodogram of PC1 (a), PC2 (b), and PC3 (c).

Figure 4 shows the magnitude of the eigenvalue spectra of the three main EOF patterns generated. The important time scales are shown along the x-axis representing the 4 monthly, semi-annual, annual, and interannual signals. The spectrum of the EOF1 pattern has a strong annual signal. The annual signal dominates the overall variability with a value more than three times the maximum of the other two main modes. The strong annual signal of Pattern EOF1 shows a strong homogeneous pattern, as also indicated by the small standard deviation of its annual cycle. The spectrum of Pattern EOF2 has strong annual and semiannual signals, with the semiannual signal being slightly stronger than that of EOF1. Interestingly, there is a signal that appears for more than a decade which may be related to decade-like scale fluctuations in the western Pacific (Hendon, 2003b; Kurniawati et al., 2020; Lestari et al., 2018). The EOF3 Region spectrum has two strong peaks and several weaker peaks. Similar to Region EOF1, the annual cycle dominates the rainfall variability of this region. From the annual cycle, there is a peak in May–July, and a smaller peak in November–January. Based on the main PC signal spectrum in Figure 3, other important signals also appear that contribute to high standard deviations in intra-seasonal and inter-annual cycles, including 4-monthly, 2-yearly, 4-yearly, 7-yearly, and 10-yearly signals, where this interannual signal is possibly a signal related to ENSO (4-7 years). Overall, all three regions show strong interannual signals. The rainfall spectrum throughout Indonesia shows the dominance of annual and semi-annual signal types with the annual signal being three times stronger than the semi-annual signal. The EOF analysis that has been carried out can be used to regionalize climate variability based on annual and inter-annual rainfall cycles. The EOF method produces clear boundaries and shows the predominance of annual signals and some semi-annual signals in the spectrum.

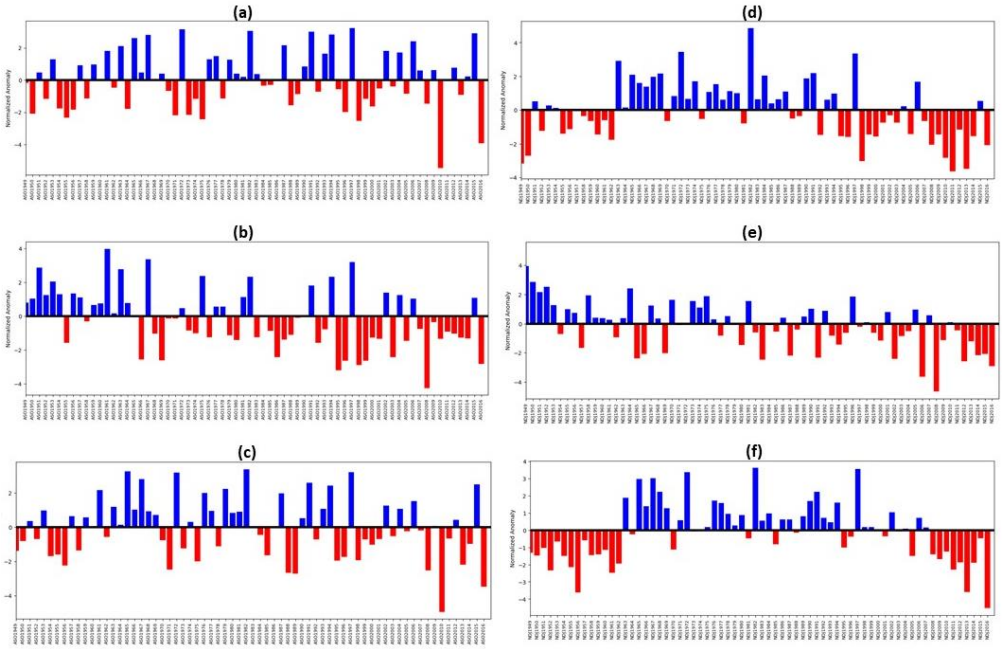

Figure 4 Normalized anomalies at ASO (left) and NDJ (right) seasons for PC1 (a, d), PC2 (b, e), and PC3 (c, f).

The variation in eigenvalues in PC1, PC2, and PC3 has almost the same pattern for each mode, but if observed using FFT analysis differences will be seen in each mode. To observe further the influence of ENSO/IOD on rainfall in Indonesia, researchers continued their observations by looking for normalized anomaly values for each main PC at the end of the dry season and the beginning of the rainy season. Figure 4 shows the normalized anomalies of PC1, PC2, and PC3 per year when the beginning of the rainy season (NDJ) and the end of the dry season (ASO) occur in each main EOF mode. The PC2 and PC3 values during the ASO season have a positive trend, indicating that there is an increase in rainfall throughout the observation period, while the PC2 values tend to decrease, although not significantly. Similar results were also shown for each major PC in the NDJ season. The PC1 and PC2 values show a positive trend while PC3 is negative. The different trends shown by PC1 and PC3 allow for the influence of ENSO and IOD. To confirm this, researchers continued observations by looking at

ENSO and IOD trends. ENSO is represented by the Niño3.4 index and IOD is observed by the Dipole Mode Index.

Researchers need to emphasize that the positive phase and negative phase in Figure 5 has not shown the rainfall deficit/surplus in the three main EOF modes. However, it only explains the statistical results of the EOF method which shows the dominance of data in the main mode in the form of fluctuations in weight changes in EOF values only. However, researchers have classified ENSO and IOD phenomena in the Pacific Ocean and Indian Ocean by referring to normalized anomaly values from calculations for five consecutive months of positive or negative DMI and Niño34 Index values from the year of observation. Guided by the normalized DMI and Niño3.4 anomaly calculations, the positive and negative phase fluctuations in Figure 4 could be compared with Figure 5 as an illustration of the impact of the ENSO and IOD phenomena on rainfall in Indonesia. The normalized anomaly graph of Niño3.4 and DMI could be observed in Figure 5.

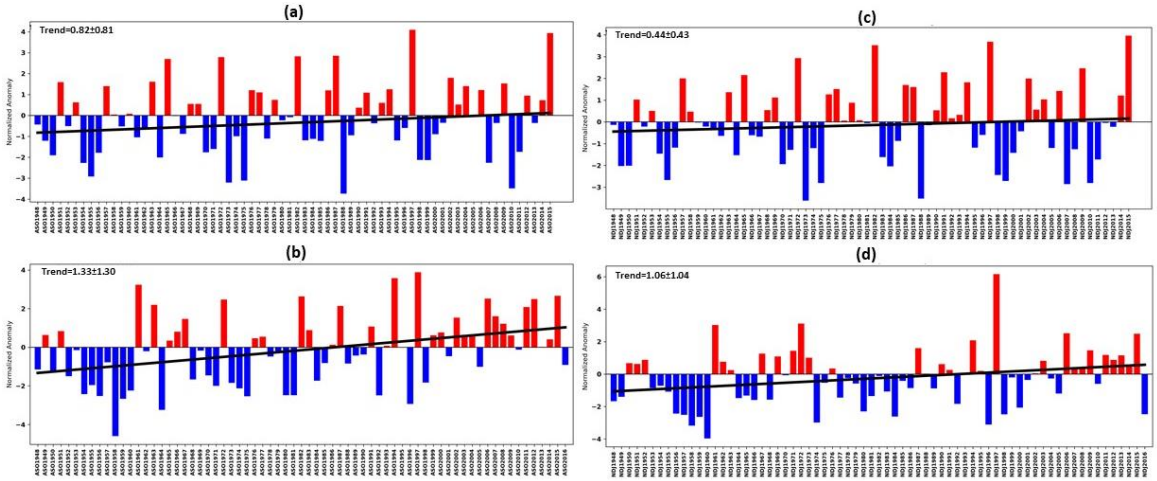

Figure 5 Normalized Anomalies from 1948-2016 in the ASO (left) and NDJ (right) seasons for Niño3.4 (a, c) and DMI (b, d).

Differences in the topography of the pattern in the mapping results of each EOF mode cause variations in rainfall at the end of the ASO dry season and the beginning of the NDJ rainy season. Based on previous research, Hamada et al., (2002) stated that the rainy season tends to be delayed in El Niño years. This is in line with the results of this study that rainfall deficits were recorded in the three main EOF modes as shown in Figure 4, especially in the EOF1 pattern which has many highlands and lowlands as also described by Jun-Ichi et al., (2012). Based on the climatology results in Figure 3 and clarified in Figure 4, the results show that the EOF1 region is the area that has the highest rainfall during the rainy season and the lowest rainfall during the dry season. The EOF2 region has rainfall that tends to be stable throughout the year compared to the other two main modes. This is because EOF2 is located on the equator of the Indonesian maritime continent (Aldrian and Susanto, 2003). Researchers also observed that this anomaly is closely related to the ocean dynamics that occur in the Pacific Ocean (ENSO) and Indian Ocean (IOD) during the ASO and NDJ seasons as shown in Figure 4 and Figure 5. The analysis covers the large ocean around Indonesia to the Niño3 region (35°S–35°N, 40°E–120°W) to see the ENSO response. The response is seen based on the correlation value between the EOF eigenvalues during ASO and NDJ in each region with respect to SST and winds along the equatorial Indian Ocean and Pacific Ocean. Only correlation values above the 95% significance level are presented in this study. The observation results can be seen in Figure 6.

In the ASO season, there is a significant positive correlation between PC1 and local SST (<-0.8) in the Indian Ocean adjacent to Indonesia, from the South China Sea to the Banda Sea. The pattern shows a relationship with the Asian winter monsoon and the location of the ITCZ. There is a positive correlation for some parts of the central Pacific in the NDJ season. In the ASO, a significant negative correlation exists in the northwest Pacific Ocean, the map shows two dipoles of correlation values. The

first dipole is shown by the opposite correlation between the maritime continent (positive) and the equatorial Indian Ocean (negative), and the other dipole is between the maritime continent and the western part of the equatorial Pacific Ocean. Negative correlations exist in the warm pool area, northeastern Indonesia and the ITCZ. Negative correlations exist for significant Niño3 patterns and parts of the Indian Ocean. During the ASO season, this dipole is stronger than during the NDJ season, with correlation values above 0.8. In general, the EOF1 pattern experiences a positive local SST influence on rainfall but also a strong negative influence from ENSO and IOD in the ASO season. The response to these two phenomena was stronger at the end of the dry season in Indonesia.

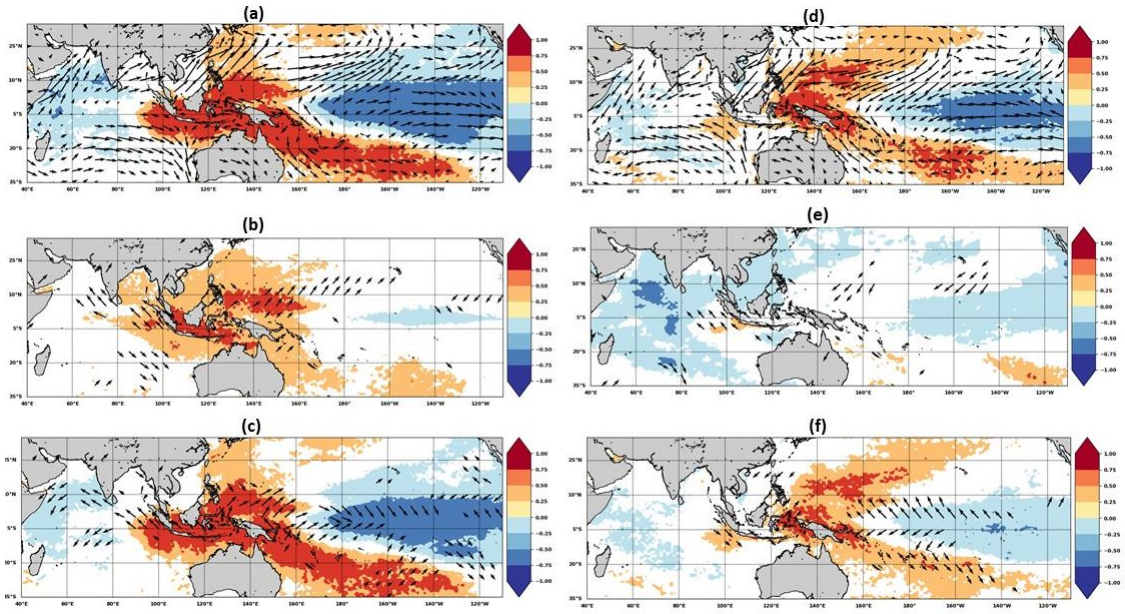

Figure 6 Simultaneous correlation of average rainfall for each EOF mode with SST and 850 hPa winds for ASO (left) and NDJ (right) seasons for PC1 (a, d), PC2 (b, e), and PC3 (c, f). Areas above the 95% confidence level are colored for SST and zonal or meridional winds.

The EOF2 pattern shows weaker PC2 responses to SST and wind than PC1. There are only some very positive responses to SST in the western Pacific during the ASO season. A very weak spatial pattern appears for the NDJ season, the pattern is different from EOF1 which is negative while in EOF2 it is positive although the response is very weak. Likewise, the response to the western Indian Ocean. The results are consistent with the analysis of SST in the Indian Ocean, which is positive. The EOF2 pattern responds very weakly to ENSO and IOD compared to EOF1. Meanwhile, the response of PC3 in ASO and NDJ seasons in the EOF3 pattern to SST can also be observed in Figure 6. There is a significant signal of western equatorial Pacific and Indian Ocean in NDJ season. The distribution of the response in NDJ is almost as wide and strong as the EOF1 pattern. The ENSO response in the ASO season is almost the same pattern as EOF1, although slightly weaker. The signal was stronger in ASO than in NDJ. In ASO, the spatial pattern shows a smaller positive area compared to the EOF1 Pattern. Thus, the EOF1 Pattern is more strongly affected by ENSO in ASO than the EOF3 Pattern.

In general, the ASO seasons are the most responsive seasons, with the most significant correlation values in all three major PC patterns. The PC values in EOF1 and EOF3 patterns respond negatively to ENSO events with a significance greater than -0.85 from August to October. Confirmation of seasonality or variation of monthly rainfall in all patterns during ENSO events needs further investigation. The high correlation of the ASO season in most parts of Indonesia can be used as a reference to predict the climate in Indonesia by looking at the response of rainfall to ENSO and IOD. Haylock & McBride, (2001) showed the relationship of Indonesia-wide rainfall index (63 stations) to Southern Oscillation Index (SOI) values during 1950-1998, rainfall during the DJF season in Indonesia is essentially unpredictable. Nicholls (1981) presented evidence that interannual fluctuations in early

monsoon rainfall over the Indonesian archipelago can be well predicted from atmospheric pressure anomalies.

Analyses by previous studies suggest that Indonesian rainfall is spatially strongly associated with ENSO, which peaks between September and November. Figure 7 shows the results of analyses of mean SST anomalies overlaid with zonal and meridian winds at the 850 hPa level. During El-Niño/positive IOD, warm SST anomalies are seen to the east of the Tropical Pacific Ocean (TPO). While cold SST anomalies were detected west of the TPO (Indonesian waters). The maximum intensity of the negative SST anomaly around Indonesian waters occurs during the ASO season. The negative anomaly creates a difference in temperature gradient between Indonesian waters and the eastern part of the TPO, causing the formation of westerly winds in the TPO. This change in wind direction causes a shift of the warm water pool to the east of the TPO, reducing convective activity over Indonesia. As a result, Indonesia experienced a rainfall deficit during this phenomenon.

Meanwhile, during the La-Niña event, the maximum intensity of the SST anomaly was around 0.7°C. This highest SST anomaly was also centered over southern Java. This positive SST anomaly triggered increased convective activity over Indonesia. However, it is slightly away from the southern coastal area of Java. This positive SST anomaly triggers increased convective activity over Indonesia, causing an increase in rain intensity over this pattern.

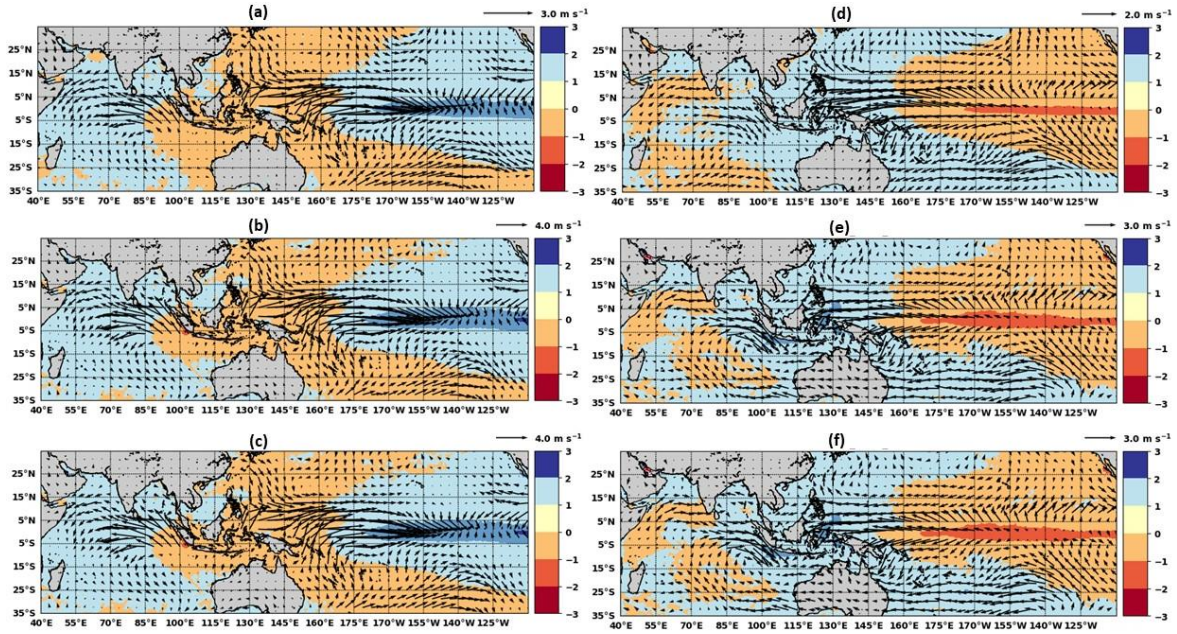

Figure 7. Map of average SST anomalies, superimposed with wind anomalies at the 850 hPa level (m/s; vector) at the ASO seasons during El-Niño (a), Simultaneous El Niño and Positive IOD (b), Positive IOD (c), La Niña (d), Simultaneous La Niña and Negative IOD (e), and Negative IOD (f).

Figure 8 shows the average SST anomaly overlaid with 850 hPa level wind anomaly during El-Niño/La-Niña and Positive/Negative IOD events at the NDJ seasons. During the El-Niño /positive IOD formation phase, negative SST anomalies began to be observed in Indonesian waters although with a low intensity ranging from 0.2 °C to 0.4 °C. This cold-water mass tends to be centered around the Indonesian pattern in the central BBS (southern waters of Kalimantan and Nusa Tenggara Islands). Meanwhile, due to the weakening of the west wind in the Indian Ocean, the water mass in the eastern Indian Ocean becomes colder than the western Indian Ocean (Indonesian waters). Furthermore, this change triggers circulation changes in the atmosphere. Easterly winds begin to be observed in the tropical Indian Ocean. When entering the ASO season, which is the peak of the positive IOD phenomenon, the east wind moving from the southern waters of Indonesia becomes very strong. This movement is accompanied by the movement of warm water masses to the west of the Indian Ocean. It is then replaced by cold water masses in the lower layers of Indonesian waters. Therefore, the observed negative SST anomaly is getting higher >-1.5 °C.

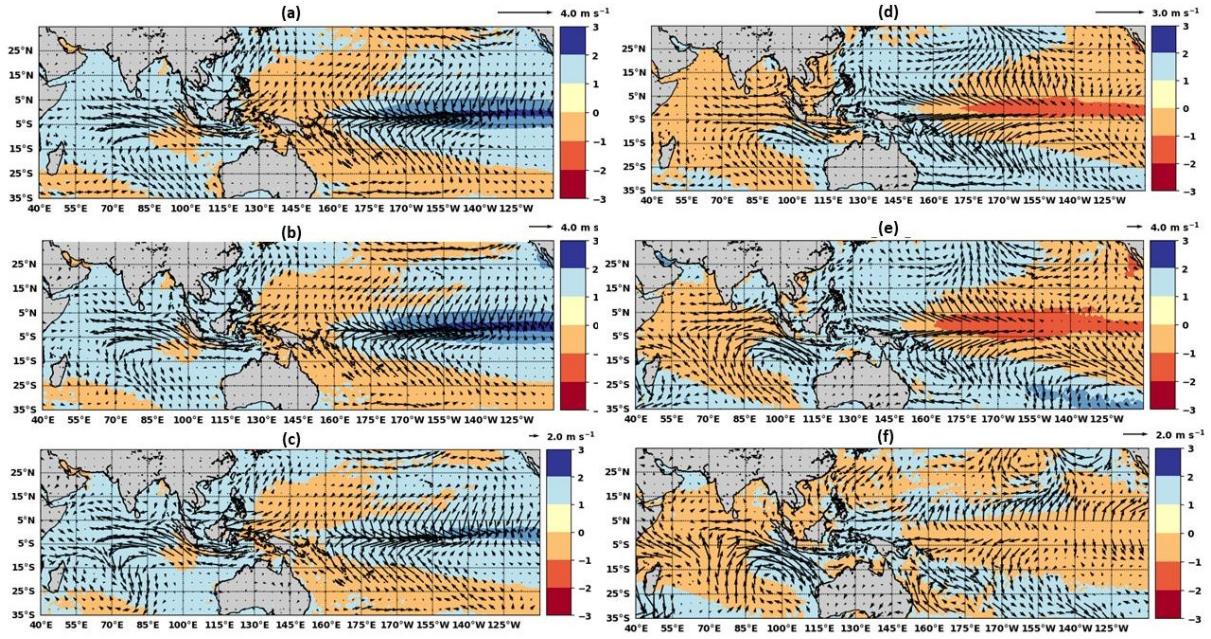

Figure 8 Map of average SST anomalies, superimposed with wind anomalies at the 850 hPa level (m/s; vector) at the NDJ seasons during El-Niño (a), Simultaneous El Niño and Positive IOD (b), Positive IOD (c), La Niña (d), Simultaneous La Niña and Negative IOD (e), and Negative IOD (f).

Different ocean-atmosphere interaction conditions occurred during the negative IOD and La Niña phenomena. SST anomalies observed in the western Indian Ocean and eastern Pacific Ocean are cooler than SST anomalies in the southeastern Indian Ocean and Indonesian waters. During the negative IOD formation phase, the west wind blowing towards Indonesian waters is getting stronger. The warm water mass in the eastern Indian Ocean moves to Indonesia, strengthening the SST difference gradient in the eastern and southeastern Indian Ocean. Then, it encourages high convection activity in Indonesian waters as a result of warmer Indonesian waters. However, from Figure 8 it could be seen that the intensity of SST warming in the Eastern Indian Ocean decreases during the ASO season. This was thought to be influenced by the shift in monsoon activity observed from the movement of the SST anomaly. During the negative IOD, the SST anomaly in Indonesian waters is warmer than during the La Niña event. During the negative IOD, the maximum intensity of positive SST anomaly in Indonesian waters reached +1.0 °C. The highest positive SST anomaly was centered south of Java Island. This condition confirms the high positive rainfall anomaly in southern Sumatra and Java (Yamagata & Masumoto, 1992; Zheng, 2019).

Figures 9 (a) and (b) illustrate the average vertical velocity in the ASO and NDJ seasons during positive/negative IOD and El Niño/La Niña. During El Niño and Positive IOD, two dipoles are observed in the tropical Indian Ocean, with the positive area centered over Indonesia and two negative areas centered over the western Indian Ocean and central Pacific Ocean. The intensity of the positive area decreases and even disappears during the NDJ monsoon season. The negative area around Indonesia strengthens and the branch of the positive area in the Indian Ocean expands. This pattern is related to the spatial distribution of SST anomalies during this climate anomaly event. Cooler SSTs triggered low-level wind divergence and reduced evaporation, resulting in decreased convective activity over Indonesia. As a result, rainfall in the Indonesian pattern decreased significantly. This result is in accordance with previous studies which stated that the positive IOD phenomenon alters atmospheric circulation and causes rainfall surplus in eastern Africa and rainfall deficit in Indonesia (Ashok et al., 2004).

Meanwhile, the average vertical velocity anomalies during negative IOD and La Niña events are shown in Figure 9. During negative IOD events, negative dipole areas dominate the Indonesian pattern, especially during the NDJ season. The positive area is centered over the western tropical Indian Ocean. This anomaly indicates the strengthening of convective activity in the eastern Indian Ocean. This

condition triggers convergence in the Indonesian pattern and increases the occurrence of convective activity in the Indonesian pattern.

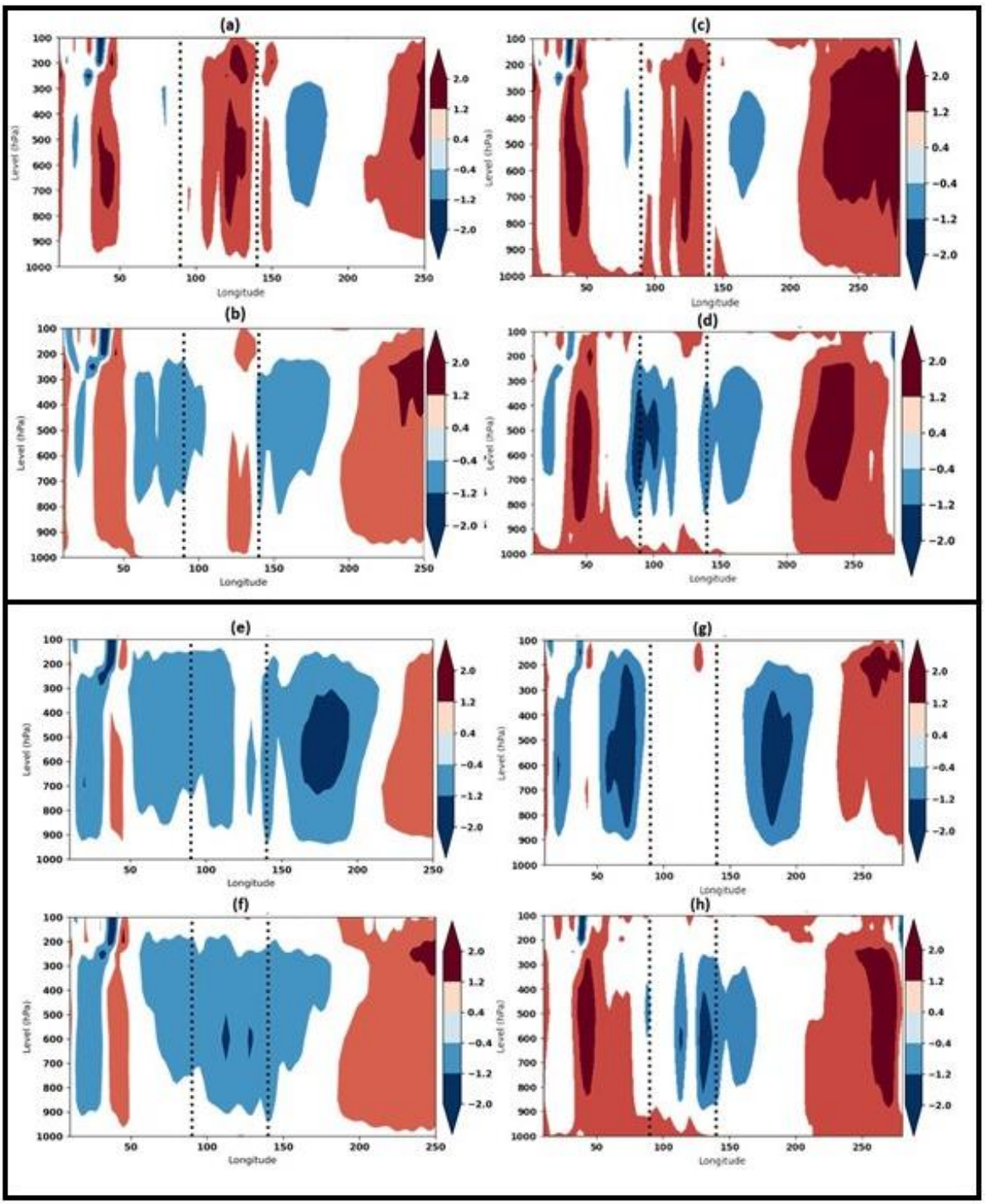

Figure 9 Composite map of vertical velocity anomalies during the ASO (up) and NDJ (bottom) seasons for El-Niño (a, e), La Niña (b, f), Positive IOD (c, g), and Negative IOD (d, h).

The magnitude of the impact of SSTs and winds at the end of the dry season (ASO) and the beginning of the rainy season (NDJ) has been discussed. Warmer SSTs surround the Indonesian Maritime Continent and the South Pacific Convergence, and cooler SSTs are located in the Niño3.4

pattern and the western Indian Ocean. A decrease in normal rainfall is detected in each PC in the dry season (ASO) which tends to coincide with warmer SSTs in the central Pacific. Local SST around the Indonesian maritime continent has decreased and has warmed in the western Indian Ocean. Rainfall is also positively correlated with zonal winds across Java and the surrounding seas. In contrast, rainfall in each EOF PC in the Indonesian Pattern during the wet season (NDJ) tends to be unrelated to SST around the Indonesian equator. However, rainfall is negatively correlated with subtropical SST in both hemispheres. The results of the correlation of average rainfall in the EOF1 pattern with SST are in line with previous studies based on broader pattern averages for southern Indonesia or the whole pattern (Chang et al., 2004; Irfan et al., 2022). In general, the relationship between local SST and rainfall emerges in EOF1 and EOF3 patterns and is less clear in EOF2. It is important to further investigate other atmospheric factors that regulate rainfall patterns in the EOF2 pattern because the study area is a maritime continent surrounded by highly variable and volatile oceans, so it needs further observation of other climate parameters that affect it.

4. CONCLUSION

The EOF method is effective for investigating rainfall variability in the Indonesian pattern. Rainfall types in Indonesia can be divided into three patterns that have different climatic characteristics. The study was conducted by analyzing the spatial patterns and time series spectra of the generated EOF main modes. The results provided strong 12-monthly and 6-monthly signals and showed an inter-annual cycle caused by the influence of ENSO/IOD. Rainfall variability in the Indonesian pattern was observed based on the results of EOF analysis and its response to IOD and ENSO events. A strong negative rainfall response is found in the EOF1 and EOF3 patterns to ENSO/IOD in the Niño3 pattern at the end of the dry season (ASO) and weakens at the beginning of the rainy season (NDJ). The negative correlation allows a decrease in rainfall in Indonesia and is exacerbated during the dry season, causing drought and increasing the threat of hydrometeorological disasters. In contrast, during La Niña/Negative IOD, or cold phase, rainfall in Indonesia has experienced a large increase throughout the year both at the end of the dry season (ASO) and the beginning of the rainy season (NDJ). ENSO's influence on rainfall in Indonesia only lasts until November, although some parts of the world may still be impacted. Surprisingly, the EOF2 pattern experiences a much weaker ENSO impact than the other two patterns.

Drought conditions in the dry season generally arise in years of positive IOD and concurrent El Niño events. In addition, abundant rainfall tends to occur in negative IOD years and La Niña years. On the other hand, rainfall in Indonesia tends to be unrelated to ENSO/IOD rainfall at the beginning of the rainy season (NDJ). Based on observations, severe drought conditions occurred in three El Niño years that coincided with positive IOD, namely 1982, 1987, 1997, 2002, and 2015, and on the contrary, the worst wet conditions occurred in two La Niña years and negative IOD that coincided, namely 1950, 1985, 1998, and 2010. The observations show that rainfall in Indonesia is closely related to the dynamics of ocean-atmosphere interaction in the Indo-Pacific pattern. Rainfall anomalies in Indonesia are closely related to the ENSO/IOD interannual cycle. The results of this study are expected to provide a reference and a clear picture of the characteristics of climate types in Indonesia. This study can be used as a reference to predict annual and interannual cycles caused by ocean and atmospheric dynamics surrounding the Indonesian archipelago. This study serves as a guideline in taking preventive actions to deal with the threat of hydrometeorological disasters that are prone to occur in Indonesia, such as floods, long droughts, forest and peatland fires, and haze disasters.

ACKNOWLEDGEMENT

This research is part of the first author's dissertation. We would like to thank Sriwijaya University for supporting this research activity through the Chancellor's Assistance Scholarship for the first author. We also say thanks to the Meteorology, Climatology, and Geophysics Agency of Indonesia for providing SACA&D rainfall data.

REFERENCE

Aldrian, E. (2001). Pembagian Iklim Indonesia Berdasarkan Pola Curah Hujan Dengan Metoda " Double Correlation ." *Jurnal Sains & Teknologi Modifikasi Cuaca*, *2*(1), 2–11.

Aldrian, E., & Dwi Susanto, R. (2003). Identification of three dominant rainfall regions within Indonesia and their relationship to sea surface temperature. *International Journal of Climatology*, *23*(12), 1435–1452. https://doi.org/10.1002/joc.950

Ardiani, N. (2013). *Penggunaan empirical orthogonal function (eof) untuk identifikasi karakteristik curah hujan (studi kasus: das ciujung-cidurian)*.

Ashok, K., Guan, Z., & Yamagata, T. (2003). Influence of the Indian Ocean Dipole on the Australian winter rainfall. *Geophysical Research Letters*, *30*(15), 3–6. https://doi.org/10.1029/2003GL017926

Chang, C. P., Wang, Z., Ju, J., & Li, T. (2004). On the relationship between western maritime continent monsoon rainfall and ENSO during northern winter. *Journal of Climate*, *17*(3), 665–672. https://doi.org/10.1175/1520-0442(2004)017<0665:OTRBWM>2.0.CO;2

Field, R. D., Van Der Werf, G. R., Fanin, T., Fetzer, E. J., Fuller, R., Jethva, H., Levy, R., Livesey, N. J., Luo, M., Torres, O., & Worden, H. M. (2016). Indonesian fire activity and smoke pollution in 2015 show persistent nonlinear sensitivity to El Niño-induced drought. *Proceedings of the National Academy of Sciences of the United States of America*, *113*(33), 9204–9209. https://doi.org/10.1073/pnas.1524888113

Hamada, J. I., Yamanaka, M. D., Matsumoto, J., Fukao, S., Winarso, P. A., & Sribimawati, T. (2002). Spatial and temporal variations of the rainy season over Indonesia and their link to ENSO. *Journal of the Meteorological Society of Japan*, *80*(2), 285–310. https://doi.org/10.2151/jmsj.80.285

Hamada, Y., Tsuji, N., Kojima, Y., Qirom, M., Sulaiman, A., Firmanto, Jagau, Y., Irawan, D., Naito, R., & Nirmala Sari, E. (2016). *Guidebook for estimating carbon emissions from tropical peatlands in Indonesia*. 47.

Haylock, M., & McBride, J. (2001). Spatial coherence and predictability of Indonesian wet season rainfall. *Journal of Climate*, *14*(18), 3882–3887. https://doi.org/10.1175/1520-0442(2001)014<3882:SCAPOI>2.0.CO;2

Hendon, H. H. (2003a). Indonesian rainfall variability: Impacts of ENSO and local air-sea interaction. *Journal of Climate*, *16*(11), 1775–1790. https://doi.org/10.1175/1520-0442(2003)016<1775:IRVIOE>2.0.CO;2

Hendon, H. H. (2003b). Indonesian rainfall variability: Impacts of ENSO and local air–sea interaction. *Journal of Climate*, *16*(11), 1775–1790.

Horii, T., Siswanto, E., Iskandar, I., Ueki, I., & Ando, K. (2022). Can Coastal Upwelling Trigger a Climate Mode? A Study on Intraseasonal-Scale Coastal Upwelling Off Java and the Indian Ocean Dipole. *Geophysical Research Letters*, *49*(15), e2022GL098733.

Irfan, M., & Iskandar, I. (2022). the Impact of Positive Iod and La Niña on the Dynamics of Hydro-Climatological Parameters on Peatland. *International Journal of GEOMATE*, *23*(97), 115–122. https://doi.org/10.21660/2022.97.3307

Irfan, M., Safrina, E., Koriyanti, E., Saleh, K., Kurniawaty, N., & Iskandar, I. (2022). What are the dynamics of hydrometeorological parameters on peatlands during the 2019 extreme dry season? *Journal of Physics: Conference Series*, *2165*(1), 0–6. https://doi.org/10.1088/1742-6596/2165/1/012003

Iskandar, I., Lestari, D. O., Saputra, A. D., Setiawan, R. Y., Wirasatriya, A., Susanto, R. D., Mardiansyah, W., Irfan, M., Rozirwan, Setiawan, J. D., & Kunarso. (2022). Extreme Positive Indian Ocean Dipole in 2019 and Its Impact on Indonesia. *Sustainability (Switzerland)*, *14*(22), 1–15. https://doi.org/10.3390/su142215155

Iskandar, I., Sari, Q. W., Setiabudiday, D., Yustian, I., & Monger, B. (2017). The distribution and variability of chlorophyll-a bloom in the southeastern tropical Indian ocean using empirical orthogonal function analysis. *Biodiversitas*, *18*(4), 1546–1555. https://doi.org/10.13057/biodiv/d180433

Iskandar, I., Tozuka, T., Masumoto, Y., & Yamagata, T. (2008). Impact of Indian Ocean Dipole on intraseasonal zonal currents at 90°E on the equator as revealed by self-organizing map. *Geophysical Research Letters*, *35*(14), 1–5. https://doi.org/10.1029/2008GL033468

Jun-Ichi, H., Mori, S., Kubota, H., Yamanaka, M. D., Haryoko, U., Lestari, S., Sulistyowati, R., & Syamsudin, F. (2012). Interannual rainfall variability over northwestern Jawa and its relation to the Indian Ocean Dipole and El Niño-Southern Oscillation events. *Scientific Online Letters on the Atmosphere*, *8*(1), 69–72. https://doi.org/10.2151/sola.2012-018

Kajita, R., Yamanaka, M. D., & Kozan, O. (2022). Reconstruction of rainfall records at 24 observation stations in Sumatera, Colonial Indonesia, from 1879–1900. *Journal of Hydrometeorology*, 1–71. https://doi.org/10.1175/jhm-d-20-0245.1

Kurniawati, N., Lestari, D. O., Fauziyah, Setiabudidaya, D., & Iskandar, I. (2020). Variation of thermodynamic

layers over the South Coastal Java Region (SJCR) and their influences on nutrient abundance. *Journal of Physics: Conference Series*, *1568*(1). https://doi.org/10.1088/1742-6596/1568/1/012029

Landsea, C. W., & Knaff, J. A. (2000). How much skill was there in forecasting the very strong 1997–98 El Niño? *Bulletin of the American Meteorological Society*, *81*(9), 2107–2120.

Lestari, D. O., Sutriyono, E., Kadir, S., & Iskandar, I. (2019). Impact of 2016 weak La Niña Modoki event over the Indonesian region. *International Journal of GEOMATE*, *17*(61), 156–162. https://doi.org/10.21660/2019.61.8256

Lestari, D. O., Sutriyono, E., Sabaruddin, S., & Iskandar, I. (2018). Respective Influences of Indian Ocean Dipole and El Niño-Southern Oscillation on Indonesian Precipitation. *Journal of Mathematical and Fundamental Sciences*, *50*(3), 257–272. https://doi.org/10.5614/j.math.fund.sci.2018.50.3.3

Mason, S. J., & Mimmack, G. M. (2002). Comparison of some statistical methods of probabilistic forecasting of ENSO. *Journal of Climate*, *15*(3), 8–29. https://doi.org/10.1175/1520-0442(2002)015<0008:cossmo>2.0.co;2

Pourasghar, F., Tozuka, T., Jahanbakhsh, S., Sari Sarraf, B., Ghaemi, H., & Yamagata, T. (2012). The interannual precipitation variability in the southern part of Iran as linked to large-scale climate modes. *Climate Dynamics*, *39*(9–10), 2329–2341. https://doi.org/10.1007/s00382-012-1357-5

Putra, R., Sutriyono, E., Kadir, S., Iskandar, I., & Lestari, D. O. (2019). Dynamical link of peat fires in South Sumatra and the climate modes in the Indo-Pacific region. *Indonesian Journal of Geography*, *51*(1), 18–22. https://doi.org/10.22146/ijg.35667

Ramage, C. S. (1968). Role of a tropical "maritime continent" in the atmospheric circulation. *Monthly Weather Review*, *96*(6), 365–370.

Saji, N. H., & Vinayachandran, P. N. (1999). *A dipole mode in the tropical Indian Ocean*. *401*(September), 360–364.

Sprintall, J., Chong, J., Syamsudin, F., Morawitz, W. L. M., Hautala, S., Bray, N. A., & Wijffels, S. (1999). Dynamics of the South Java Current in the Indo-Australian Basin. *Geophysical Research Letters*, *26*(16), 2493–2496. https://doi.org/10.1029/1999GL002320

Suhadi, Supari, Iskandar, I., Irfan, M., & Akhsan, H. (2023). Drought Assessment in Aceh and North Sumatra Using Effective Drought Index. *Science and Technology Indonesia*, *8*(2), 259–264. https://doi.org/10.26554/sti.2023.8.2.259-264

Tavakol, A., Rahmani, V., & Harrington, J. (2020). Evaluation of hot temperature extremes and heat waves in the Mississippi River Basin. *Atmospheric Research*, *239*(February), 104907. https://doi.org/10.1016/j.atmosres.2020.104907

Yamagata, T., & Masumoto, Y. (1992). *Interdecadel Natural Climate Variability in the Western Pacific and its Implication in Global Warming*. *February*.

Yamanaka, M. D. (2016). Physical climatology of Indonesian maritime continent: An outline to comprehend observational studies. *Atmospheric Research*, *178–179*, 231–259. https://doi.org/10.1016/j.atmosres.2016.03.017

Yamanaka, M. D. (2018). Equatorial rainfall and global climate. *ISQUAR*, *3*(March), 3–6.

Zheng, X. T. (2019). Indo-Pacific Climate Modes in Warming Climate: Consensus and Uncertainty Across Model Projections. *Current Climate Change Reports*, *5*(4), 308–321. https://doi.org/10.1007/s40641-019-00152-9